

# $B \rightarrow \pi \ell \nu_\ell$ Width and $|V_{ub}|$ from QCD Light-Cone Sum Rules

A. Khodjamirian <sup>(a)</sup>, Th. Mannel <sup>(a)</sup>, N. Offen <sup>(b)</sup> and Y.-M. Wang <sup>(a)</sup>

<sup>(a)</sup> *Theoretische Physik 1, Physik Department, Universität Siegen,  
D-57068 Siegen, Germany*

<sup>(b)</sup> *Institut für Theoretische Physik, Universität Regensburg,  
D-93040 Regensburg, Germany*

We employ the  $B \rightarrow \pi$  form factors obtained from QCD light-cone sum rules and calculate the  $B \rightarrow \pi \ell \nu_\ell$  width ( $\ell = e, \mu$ ) in units of  $1/|V_{ub}|^2$ , integrated over the region of accessible momentum transfers,  $0 \leq q^2 \leq 12.0 \text{ GeV}^2$ . Using the most recent BABAR-collaboration measurements we extract  $|V_{ub}| = (3.50^{+0.38}_{-0.33}|_{th.} \pm 0.11|_{exp.}) \times 10^{-3}$ . The sum rule results for the form factors, taken as an input for a  $z$ -series parameterization, yield the  $q^2$ -shape in the whole semileptonic region of  $B \rightarrow \pi \ell \nu_\ell$ . We also present the charged lepton energy spectrum in this decay. Furthermore, the current situation with  $B \rightarrow \tau \nu_\tau$  is discussed from the QCD point of view. We suggest to use the ratio of the  $B \rightarrow \pi \tau \nu_\tau$  and  $B \rightarrow \pi \ell \nu_\ell$  ( $\ell = \mu, e$ ) widths as an additional test of Standard Model. The sensitivity of this observable to new physics is illustrated by including a charged Higgs-boson contribution in the semileptonic decay amplitude.

PACS numbers: 13.20.He, 12.38.Lg, 11.55.Hx

# 1 Introduction

Currently, there is a tension between the two values of  $|V_{ub}|$  extracted from inclusive and exclusive semileptonic  $B$ -decays involving  $b \rightarrow u$  transition. While the inclusive analyses typically yield a central value of  $|V_{ub}|$  larger than  $4 \times 10^{-3}$ , the exclusive determinations produce central values well below this. This tension is not significant; it ranges at a level of  $3\sigma$ , but it already has created a significant amount of speculations concerning possible new physics effects. This is in contrast to the situation with  $|V_{cb}|$ , where both the inclusive as well as the exclusive determinations yield consistent values with an uncertainty of roughly 2% (for a review on  $|V_{cb}|$  and  $|V_{ub}|$  see [1]).

The theoretical description of inclusive semileptonic  $B$  decays relies on the heavy-quark expansion which has reached a mature state. Still, the situation with  $b \rightarrow u$  inclusive decays is more complicated than with the dominant  $b \rightarrow c$  ones. In order to suppress the charm background in the inclusive  $b \rightarrow u$  decays, severe phase space cuts are necessary, for which most theoretical methods cannot rely on the heavy quark expansion based on the local operator-product expansion. The heavy quark expansion for this case uses non-local matrix elements corresponding to the light-cone distribution functions of the  $B$  meson, which also appear e.g., in the radiative  $b \rightarrow s$  decays. Due to this more complicated structure of the expansion, it is quite hard to estimate subleading terms in the heavy-quark expansion for  $b \rightarrow u$  decays. In particular the inclusive method has been scrutinized for a missing systematic effect like e.g., “weak annihilation”, however, no missing pieces could be identified yet. Still, it is believed that this method allows a determination of  $|V_{ub}|$  at a precision of a little better than 10%.

As far as exclusive decays are concerned, heavy-quark symmetries restrict the form factors for the heavy-light  $b \rightarrow u$  transitions much weaker than the ones for the  $b \rightarrow c$  transitions. Hence, the determination of  $|V_{ub}|$  from exclusive decays such as  $B \rightarrow \pi \ell \bar{\nu}$  and  $B \rightarrow \rho \ell \bar{\nu}$  requires a QCD calculation of the relevant hadronic form factors. State-of-the-art calculations do not rely on quark models any more, since the latter cannot be directly related to QCD. Already for many years, the form factors are obtained, on one hand, from lattice simulations and, on the other hand, from QCD sum rules. The two approaches are complementary: While the lattice techniques can calculate close to the maximal leptonic momentum transfer  $q^2$ , the QCD sum rule approach works best for small  $q^2$ . Extrapolating both predictions to the full phase space yields consistent results and hence there is some confidence that the form factors, in particular, for  $B \rightarrow \pi \ell \bar{\nu}$  are known with an uncertainty of 10-15%.

Currently,  $B \rightarrow \pi l \nu_l$  is the most reliable exclusive channel to extract  $|V_{ub}|$ . There is a steady progress in measuring the branching fraction and  $q^2$ -distribution for  $l = \mu, e$  (see [2, 3, 4] for the latest results). The hadronic vector form factor  $f_{B\pi}^+(q^2)$  and its scalar

counterpart  $f_{B\pi}^0(q^2)$  relevant for this decay are defined as <sup>1</sup>

$$\begin{aligned}\langle \pi^+(p) | \bar{u} \gamma_\mu b | \bar{B}^0(p+q) \rangle &= f_{B\pi}^+(q^2) \left[ 2p_\mu + \left( 1 - \frac{m_B^2 - m_\pi^2}{q^2} \right) q_\mu \right] \\ &+ f_{B\pi}^0(q^2) \frac{m_B^2 - m_\pi^2}{q^2} q_\mu,\end{aligned}\quad (1)$$

where  $f_{B\pi}^+(0) = f_{B\pi}^0(0)$ . The most recent lattice QCD computations with three dynamical flavours [5, 6] predict these form factors at  $q^2 \geq 16 \text{ GeV}^2$ , in the upper part of the semileptonic region  $0 \leq q^2 \leq (m_B - m_\pi)^2 \simeq 26.4 \text{ GeV}^2$ , with an accuracy reaching 10%. There are also recent results available [7] in the quenched approximation on a fine lattice. QCD light-cone sum rules (LCSR) with pion distribution amplitudes (DA's) allow one to calculate the  $B \rightarrow \pi$  form factors [8, 9, 10, 11, 12] at small and intermediate momentum transfers,  $0 \leq q^2 \leq q_{max}^2$ , where the choice of  $q_{max}^2$  varies between 12 and 16  $\text{GeV}^2$ .

The main goal of this paper is to present an updated LCSR prediction for the width of  $B \rightarrow \pi \ell \nu_\ell$  ( $\ell = e, \mu$ ) which is then used to extract  $|V_{ub}|$ . This work complements [12] where LCSR for  $f_{B\pi}^+$  and  $f_{B\pi}^0$  were rederived, employing the  $\overline{MS}$  scheme for the virtual  $b$ -quark in the correlation function. In [12], the shape of the form factor  $f_{B\pi}^+(q^2)$  predicted from LCSR was fitted to the earlier BABAR measurement [13] of the  $q^2$ -distribution in  $B \rightarrow \pi \ell \nu_\ell$ . In this way, some input parameters of LCSR were constrained, allowing one to decrease the theoretical uncertainty of the value  $f_{B\pi}^+(0)$ , the main prediction of [12].

In this paper, we follow a different strategy. The intervals of the Gegenbauer moments of the pion twist-2 DA are constrained using the LCSR for the pion electromagnetic (e.m.) form factor at spacelike momentum transfers. The calculated form factor is then fitted to the available experimental data on this form factor. We also slightly update the other input parameters, and recalculate the form factors  $f_{B\pi}^+(q^2)$  and  $f_{B\pi}^0(q^2)$  at  $0 \leq q^2 < q_{max}^2$  from LCSR. Our main prediction is the integral:

$$\Delta\zeta(0, q_{max}^2) \equiv \frac{G_F^2}{24\pi^3} \int_0^{q_{max}^2} dq^2 p_\pi^3 |f_{B\pi}^+(q^2)|^2 = \frac{1}{|V_{ub}|^2 \tau_{B^0}} \int_0^{q_{max}^2} dq^2 \frac{d\mathcal{B}(B \rightarrow \pi \ell \nu_\ell)}{dq^2}, \quad (2)$$

where  $p_\pi = \sqrt{(m_B^2 + m_\pi^2 - q^2)^2/4m_B^2 - m_\pi^2}$  is the pion 3-momentum in the  $B$ -meson rest frame, and the above equation is valid for  $\ell = e, \mu$  in the limit  $m_l = 0$ . As in [12], the value  $q_{max}^2 = 12.0 \text{ GeV}^2$  is adopted. The predicted  $\Delta\zeta(0, 12 \text{ GeV}^2)$  is used to extract  $|V_{ub}|$  from the most recent BABAR-collaboration results [2, 3] for the measured partial branching fraction integrated over the same  $q^2$ -region. Furthermore, we predict the form factors in the whole semileptonic region by fitting the LCSR results at  $q^2 \leq q_{max}^2$  to the  $z$ -series parameterization in the form suggested in [14]. In addition to the  $q^2$ -distribution of the width, we present a “by-product” observable: the lepton energy spectrum in  $B \rightarrow \pi \ell \nu_\ell$ . Finally, we calculate the ratio of the  $B \rightarrow \pi \tau \nu_\tau$  and  $B \rightarrow \pi \ell \nu_\ell$

<sup>1</sup>Throughout this paper, we assume isospin symmetry for  $B^0$  and  $B^\pm$  semileptonic decays and consider the  $\bar{B}^0 \rightarrow \pi^+ \ell^- \bar{\nu}_\ell$  mode for definiteness, denoting it as  $B \rightarrow \pi \ell \nu_\ell$  for brevity.

( $\ell = e, \mu$ ) widths, which is independent of  $|V_{ub}|$  and in Standard Model (SM) is fully determined by the ratio  $f_{B\pi}^0(q^2) / f_{B\pi}^+(q^2)$ . We also discuss the current tension between the SM prediction and measurements of the leptonic  $B \rightarrow \tau \nu_\tau$  width, and suggest to use the semileptonic decay  $B \rightarrow \pi \tau \nu_\tau$  decay, originating from the same flavour-changing interaction, as an additional indicator of new physics. As an illustrative example, we consider the influence of a charged Higgs-boson exchange on the  $B \rightarrow \pi \tau \nu_\tau$  width.

In what follows, a brief outline of the LCSR method for  $B \rightarrow \pi$  form factors is given in Sect. 2. The choice of the Gegenbauer moments of the pion DA is discussed in Sect. 3. In Sect. 4 we present our numerical results for the form factors and for the integrated width. In Sect. 5 we discuss the  $z$ -series parameterization and present our predictions for the whole semileptonic region. In Sect. 6 we discuss the current situation with  $B \rightarrow \tau \nu_\tau$  and the decay  $B \rightarrow \pi \tau \nu_\tau$ , concluding in Sect. 7.

## 2 Outline of the method and input

To obtain the LCSR for the form factors  $f_{B\pi}^+$  and  $f_{B\pi}^0$  one uses the correlation function

$$\begin{aligned} F_\mu(p, q) &= i \int d^4x e^{iq \cdot x} \langle \pi^+(p) | T \{ \bar{u}(x) \gamma_\mu b(x), m_b \bar{b}(0) i \gamma_5 d(0) \} | 0 \rangle \\ &= F(q^2, (p+q)^2) p_\mu + \tilde{F}(q^2, (p+q)^2) q_\mu, \end{aligned} \quad (3)$$

of the  $b \rightarrow u$  vector current and the  $B$ -meson interpolating current. As explained e.g., in [12], the product of the quark operators in the above is expanded near the light-cone, provided both external momenta are highly-virtual:  $(p+q)^2, q^2 \ll m_b^2$ . The operator-product expansion (OPE) result for the invariant amplitudes in (3) is obtained in a (schematic) form:

$$F^{OPE}(q^2, (p+q)^2) = \sum_t \int \mathcal{D}u_i T^{(t)}(q^2, (p+q)^2, u_i, \bar{m}_b, \alpha_s, \mu_f) \varphi_\pi^{(t)}(u_i, \mu_f), \quad (4)$$

with a similar expression for  $\tilde{F}^{(OPE)}$ . In the above, the pion light-cone DA's  $\varphi_\pi^{(t)}(u_i)$  of growing twist  $t = 2, 3, 4$  are defined as functions of the light-cone momentum fractions  $u_i$ ; for the two-particle DA's  $u_1 = u$ ,  $u_2 = 1 - u \equiv \bar{u}$ , with the integration over  $u$ . The DA's are convoluted with the coefficient functions (hard-scattering amplitudes)  $T^{(t)}$  and  $\tilde{T}^{(t)}$  at the factorization scale  $\mu_f$ . The currently accessible approximation for the light-cone OPE includes the contributions of all two- and three-particle DA's up to the twist 4. For the leading twist-2 and twist-3 contributions the coefficient functions are calculated in NLO, taking into account the  $O(\alpha_s)$  gluon radiative corrections. The input in the OPE (4) includes: the  $b$ -quark mass (in the  $\overline{MS}$  scheme) and QCD coupling in the coefficient functions, as well as the parameters of the universal pion DA's.

The dispersion relation for the correlation function (3) in the channel of the  $B$ -meson interpolating current with momentum  $p+q$  is then employed to access the form factors:

$$F^{OPE}(q^2, (p+q)^2) = \frac{2f_B m_B^2 f_{B\pi}^+(q^2)}{m_B^2 - (p+q)^2} + \dots, \quad (5)$$

$$\begin{aligned} \tilde{F}^{OPE}(q^2, (p+q)^2) = & \frac{f_B m_B^2}{m_B^2 - (p+q)^2} \left[ f_{B\pi}^+(q^2) \left( 1 - \frac{m_B^2 - m_\pi^2}{q^2} \right) \right. \\ & \left. + f_{B\pi}^0(q^2) \frac{m_B^2 - m_\pi^2}{q^2} \right] + \dots, \end{aligned} \quad (6)$$

where  $f_B = \langle \bar{B} | m_b \bar{b} i \gamma_5 d | 0 \rangle / m_B^2$  is the  $B$ -meson decay constant. The ellipses in the above relations indicate the integrals over the spectral densities of excited and continuum  $B$ -states, for which the quark-hadron duality ansatz is used. More specifically, one approximates the higher-state contributions in (5) and (6) by the integrals over the spectral density of the calculated invariant amplitudes  $Im_{(p+q)^2} F^{OPE}(q^2, s)$  and  $Im_{(p+q)^2} \tilde{F}^{OPE}(q^2, s)$ , respectively. This approximation brings the effective threshold  $s_0^B$  into play. The final form of LCSR is obtained after applying the Borel transformation to (5) and (6) replacing the variable  $(p+q)^2$  by the Borel parameter  $M^2$ ; e.g., for the form factor  $f_{B\pi}^+$  one obtains:

$$f_{B\pi}^+(q^2) = \left( \frac{e^{m_B^2/M^2}}{2m_B^2 f_B} \right) \frac{1}{\pi} \int_{m_b^2}^{s_0^B} ds \, Im_{(p+q)^2} F^{OPE}(q^2, s) e^{-s/M^2}. \quad (7)$$

The second LCSR obtained from (6) and combined with (7) allows one to calculate the form factor  $f_{B\pi}^0(q^2)$ . Both sum rules are reliable up to  $q_{max}^2 \sim m_B^2 - 2m_b\chi$ , where  $\chi$  is some large scale, independent of  $m_b$ , so that at  $q^2 \leq q_{max}^2$  the truncated light-cone OPE can be trusted.

The interval of  $M^2$  in (7) is constrained by combining the two usual criteria for a QCD sum rule: smallness of the power corrections (here the contributions of three-particle and twist-4 DA's to  $F^{OPE}$ ), and, simultaneously, a moderate magnitude of the hadronic continuum contribution. The interval of  $s_0^B$  is constrained by equating the  $B$ -meson mass calculated from LCSR to its experimental value. Finally, the decay constant  $f_B$  is calculated from the two-point sum rule with the same  $\alpha_s$  accuracy. The explicit expressions for the amplitudes  $F^{OPE}$ ,  $\tilde{F}^{OPE}$  and their spectral functions entering LCSR, as well as a detailed description of all pion DA's entering (4), can be found in [12].

The most important contributions to the LCSR (7) originate from the twist-2 and twist-3 terms in the OPE (4). The twist-2 pion DA  $\varphi_\pi^{(2)}(u_1, u_2, \mu) = f_\pi \varphi_\pi(u, \mu)$ , is normalized to the pion decay constant  $f_\pi$ . The shape of  $\varphi_\pi(u, \mu)$  is determined by the coefficients of the Gegenbauer-polynomial expansion (Gegenbauer moments), to be discussed in the next section. In the twist-3 pion DA's, the most important input parameter is the normalization coefficient  $\mu_\pi = m_\pi^2/(m_u + m_d)$  related to the quark-condensate density. The parameters determining the shapes of the twist-3,4 DA's are known with a sufficient accuracy from the two-point QCD sum rules (see e.g., [15]).

### 3 Gegenbauer moments from the pion e.m. form factor

For the twist-2 pion DA we use the same approximation as in [12],

$$\varphi_\pi(u, \mu_f) = 6u\bar{u} \left( 1 + a_2^\pi(\mu_f) C_2^{3/2}(u - \bar{u}) + a_4^\pi(\mu_f) C_4^{3/2}(u - \bar{u}) \right), \quad (8)$$

retaining the two nonvanishing Gegenbauer moments  $a_2^\pi$  and  $a_4^\pi$  and neglecting all higher moments, so that  $a_{>4}^\pi = 0$ . This approximation is justified because the renormalization suppresses higher Gegenbauer moments at relatively large scales  $\mu_f$ , typical for the LCSR (7). The uncertainties of the input values of  $a_{2,4}^\pi(1\text{GeV})$  are larger than very small effects of the NLO evolution, which we also neglect.

In [12] these two parameters were constrained by fitting the  $B \rightarrow \pi$  form factor calculated from LCSR at different  $q^2$  to the measured shape of  $B \rightarrow \pi \ell \nu_\ell$ , yielding  $a_2^\pi(1\text{GeV}) = 0.16 \pm 0.01$  and  $a_4^\pi(1\text{GeV}) = 0.04 \pm 0.01$ , where the uncertainties only take into account the experimental error in the shape.

Here we refrain from using the  $B \rightarrow \pi \ell \nu_\ell$  data and obtain an independent constraint on the two Gegenbauer moments employing the pion e.m. form factor  $F_\pi(Q^2)$  in the spacelike region, defined as

$$\langle \pi(p+q) | j_\mu^{em} | \pi(p) \rangle = (2p+q)_\mu F_\pi(Q^2), \quad (9)$$

where  $j_\mu^{em} = \frac{2}{3}\bar{u}(x)\gamma_\mu u(x) - \frac{1}{3}\bar{d}(x)\gamma_\mu d(x)$  and  $Q^2 = -q^2$ . The LCSR for  $F_\pi(Q^2)$  derived in [16, 17] and updated in [18] is based on the correlation function, similar to (3), with virtual  $u, d$  quarks instead of the  $b$ -quark and with the axial-vector current instead of the pseudoscalar current. This sum rule has NLO accuracy in the leading twist-2 term, with the nonleading terms up to twist-6 taken into account. The  $O(\alpha_s/Q^2)$  term in LCSR correctly reproduces the large- $Q^2$  QCD asymptotics of the pion form factor, whereas the soft contributions dominate in the intermediate  $Q^2$  region. Importantly, the twist-3 contribution to the LCSR for  $F_\pi(Q^2)$  vanishes in the chiral limit. Altogether, the sum rule for the pion e.m. form factor is more sensitive to the twist-2 pion DA than the sum rules for heavy-to-light form factors. The LCSR for  $F_\pi(Q^2)$  with the currently achieved accuracy is applicable at intermediate  $Q^2$ , from  $O(1\text{GeV}^2)$  to a few  $\text{GeV}^2$ ; in the same region this form factor was accurately measured by the JLab experiment [19]. Preliminary comparison of the LCSR with these data was done in [20]. With the pion DA given by (8) and taking the remaining input from [18] we recalculated the pion e.m. form factor at  $Q^2$  in the region up to a few  $\text{GeV}^2$  as a function of  $a_2^\pi(1\text{GeV}^2)$  and  $a_4^\pi(1\text{GeV}^2)$ . As shown in Fig. 1, the result was fitted to the seven data points at  $0.6 \text{ GeV}^2 \leq Q^2 \leq 2.45 \text{ GeV}^2$ , presented in [19], yielding:

$$a_2^\pi(1 \text{ GeV}) = 0.17 \pm 0.08, \quad a_4^\pi(1 \text{ GeV}) = 0.06 \pm 0.10, \quad (10)$$

where the uncertainties include experimental errors and the variation of other input parameters taken as in [18]. We adopt these intervals for the numerical analysis of the sum rule (7), neglecting the correlation of the two uncertainties in (10). Note that the value of  $a_2^\pi$  presented above is consistent with the direct calculations of this parameter in lattice QCD [21] and from QCD sum rules [15, 22].

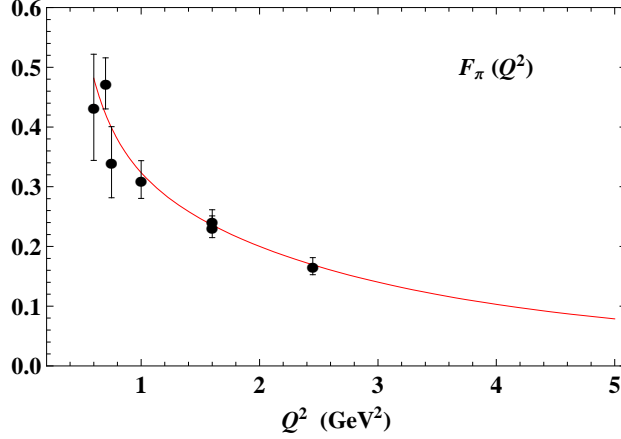


Figure 1: *The pion e.m. form factor calculated from LCSR [17, 18] as a function of Gegenbauer moments  $a_2^\pi(1 \text{ GeV})$  and  $a_4^\pi(1 \text{ GeV})$  and fitted (solid) to the experimental data points taken from [19].*

The  $\gamma^*\gamma \rightarrow \pi^0$  transition form factor, where the virtual photon has a spacelike virtuality  $Q^2$  is another important hadronic matrix element that depends on the properties of the pion DA  $\varphi_\pi(u)$ . The method [23] of combining LCSR with the dispersion relation in the photon virtuality predicts this form factor starting from  $Q^2 \sim 1 \text{ GeV}^2$ . It is important that, according to the sum rule approach, the photon-pion transition form factor contains a considerable nonperturbative soft contribution. The calculation [23] was reconsidered in [20] with the same intervals of  $a_2^\pi, a_4^\pi$  as in [12], revealing a reasonable agreement with the data at  $Q^2 \leq 15 \text{ GeV}^2$ . The most accurate LCSR analysis of the  $\gamma^*\gamma \rightarrow \pi^0$  form factor, including the new twist-6 corrections was carried out recently in [24]. It was shown that also the rise of the form factor at high- $Q^2$  observed by the BABAR collaboration [25] (albeit with large errors) can still be accommodated in the LCSR prediction at the expense of a moderate “deformation” of the shape of  $\varphi_\pi(u)$ . Most importantly, one has to increase the coefficient  $a_4^\pi(1\text{GeV})$  up to  $\sim 0.2$ , leaving  $a_2^\pi$  in the ballpark of (10) and (optionally) adding small coefficients  $a_{6,8,10}^\pi$  to the model. We illustrate the numerical influence of such variation of  $\varphi_\pi(u)$  on the  $B \rightarrow \pi$  LCSR (7) in the next section, and confirm the observation made in [24] that the heavy-light form factors are only slightly influenced by this modification of Gegenbauer moments.

The LCSR method can also be used to calculate the  $D \rightarrow \pi$  form factor. The recent analysis in [26] where the same intervals as in [12] were used revealed a very good agreement with lattice QCD and experiment. We checked that the use of broader intervals (10) does not produce a noticeable effect, simply because the twist-2 contribution is numerically less important in the  $D \rightarrow \pi$  LCSR.

## 4 Numerical results for the form factors and width

For the numerical analysis of the LCSR (7) and the related sum rule for  $f_{B\pi}^0$  we slightly updated the input used in [12]. First of all, there is practically no change of the  $b$ -quark mass. According to the last update [27], we adopt  $\bar{m}_b(\bar{m}_b) = 4.16 \pm 0.03$  GeV, conservatively inflating the quoted error by a factor of two. As explained in detail in [12], the  $\overline{MS}$ -mass of the  $b$ -quark is the most suitable mass definition for OPE of the correlation function, and the  $O(\alpha_s)$  contributions to the sum rules are comparably small. For the  $u$ - and  $d$ -quark masses entering the parameter  $\mu_\pi = m_\pi^2/(m_u + m_d)$ , we follow [26] and use the  $s$ -quark mass derived from QCD sum rules [28] and the ChPT light-quark mass ratios [29], yielding  $[m_u + m_d](2\text{GeV}) = 8.0 \pm 1.4$  MeV and, correspondingly

$$\mu_\pi(2\text{ GeV}) = 2.43 \pm 0.42\text{ GeV}, \quad (11)$$

so that the quark condensate density is  $\langle \bar{q}q \rangle(2\text{ GeV}) = -(274^{+15}_{-17}\text{ MeV})^3$ . This interval is slightly narrower, but remains within the broader range used in [12]. As already mentioned in the last section, our intervals for the parameters  $a_2^\pi$  and  $a_4^\pi$  given in (10) are broader than the ones used in [12]. The rest of the parameters determining the nonperturbative objects in the sum rules (DA's and condensate densities), as well as the conventions for the renormalization and choice of  $\alpha_s$  are taken as in [12]. As shown there, all nonasymptotic and three-particle contributions of the twist-3 DA's as well as the whole twist-4 contribution to LCSR are very small, and the uncertainties in their parameters do not produce visible changes in the numerical predictions.

The “internal” input parameters of our calculation include the renormalization scale  $\mu$ , the Borel parameters  $M$  and  $\overline{M}$ , the related duality thresholds  $s_0^B$  and  $\overline{s}_0^B$  in LCSR and in the 2-point sum rule for  $f_B$ , respectively. Here we follow the same strategy as in [12], balancing between the smallness of the subdominant contributions (twist-4 and twist-2,3 NLO terms) and a reasonable suppression of the integrals over the higher states estimated in the quark-hadron duality approximation. The only minor difference with respect to the analysis presented in [12] is that here we stay on a more conservative side, allowing for a slightly larger deviation (up to 3%) of the calculated  $B$ -meson mass from its experimental value. This leads to broader intervals for the Borel parameters and duality thresholds. More specifically, we adopt the same default renormalization scale  $\mu = 3$  GeV as in [12], allowing its variation from 2.5 to 4.5 GeV, and use in LCSR the Borel parameter range  $M^2 = (12.0 - 20.0)$  GeV<sup>2</sup>, with the threshold parameter gradually shrinking from the interval  $s_0^B = 37.5 \pm 2.5$  GeV<sup>2</sup> at  $M^2 = 12.0$  GeV<sup>2</sup> to the point  $s_0^B = 40.0$  GeV<sup>2</sup> at  $M^2 = 20.0$  GeV<sup>2</sup>. In the two-point sum rule we vary  $\overline{M}^2$  from 4.0 GeV<sup>2</sup> ( $\overline{s}_0^B = 36.5 \pm 2.5$  GeV<sup>2</sup>) to 6.0 GeV<sup>2</sup> ( $\overline{s}_0^B = 39.0$  GeV<sup>2</sup>).

The results of our calculation for  $f_{B\pi}^+(q^2)$  at  $0 < q^2 < 12.0$  GeV<sup>2</sup> are shown in Fig. 2, displaying the separate uncertainties caused by the variation of (a)  $a_2^\pi, a_4^\pi$ , (b)  $\mu_\pi$ , (c)  $\mu$ , (d)  $\{M^2, s_0^B\}$  and (e)  $\{\overline{M}, \overline{s}_0^B\}$  within the limits specified above. In addition, in Fig. 2f the default central values of the Gegenbauer moments in (10) are replaced by a model with larger  $a_4^\pi(1\text{ GeV}) = 0.22$  (model III in [24]). The small deviation of the form factor remains within our estimated uncertainty due to the  $a_2^\pi, a_4^\pi$  variation. Since we use a



narrow interval of the  $b$ -quark mass from [27], the uncertainties caused by the variation of  $\bar{m}_b$  are very small and not even visible on the plot, hence we do not show them; the remaining parameters of DA's and condensate densities generate negligibly small changes of the calculated form factors. The sensitivity to the renormalization scale is relatively large at  $q^2$  approaching  $q_{max}^2$ , and also the uncertainties due to the Borel parameter and duality threshold are now more pronounced than in [12] due to an enlargement of the adopted intervals, whereas the uncertainty due to the twist-3 normalization  $\mu_\pi$  (related to the  $u, d$  quark masses and quark condensate) decreases. The numerical results for the form factors  $f_{B\pi}^+(q^2)$  and  $f_{B\pi}^0(q^2)$  are consistent with what was obtained in [12]; a few percent shift of the central value of  $f_{B\pi}^+(0)$  (presented in Table 1 below) can be traced to the modification of the input.

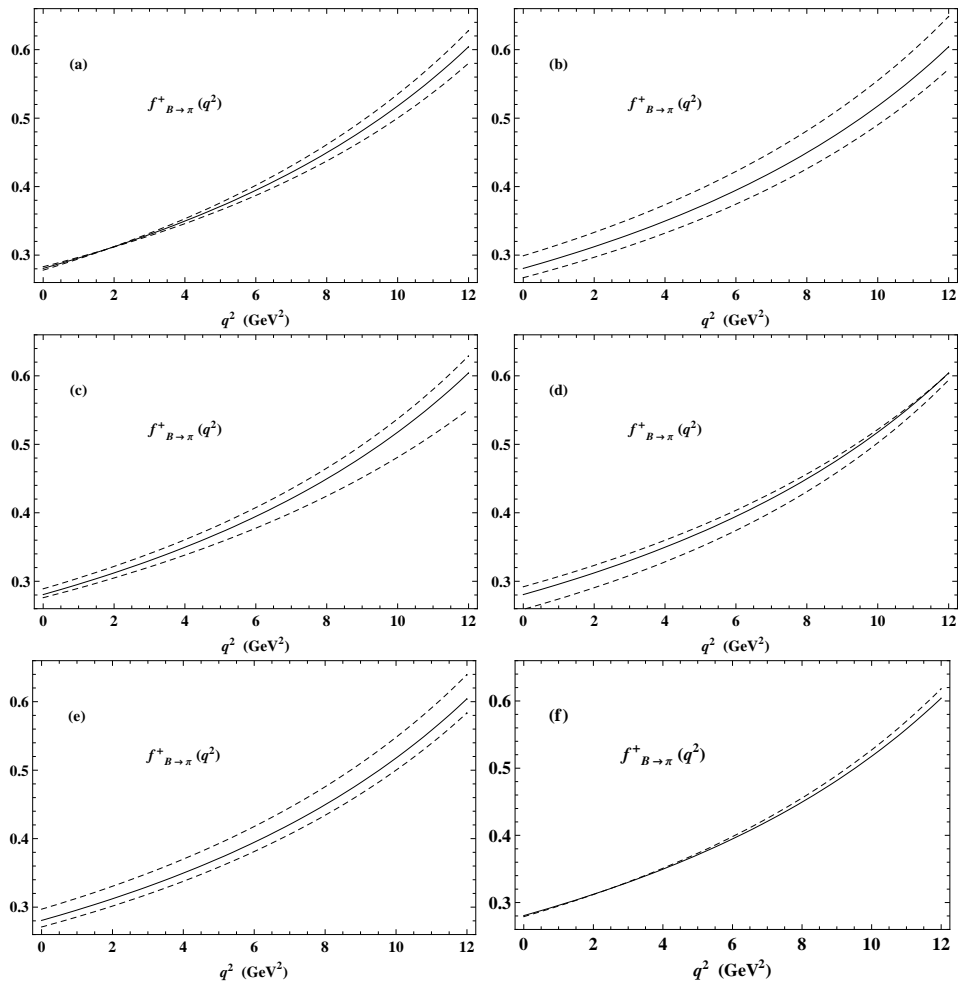


Figure 2: The form factor  $f_{B\pi}^+(q^2)$  calculated from LCSR with the central input (solid) and varying separate input parameters (dashed): (a)  $a_2^\pi, a_4^\pi$ , (b)  $\mu_\pi$ , (c)  $\mu$ , (d)  $M^2, s_0^B$  and (e)  $\overline{M}^2, \overline{s}_0^B$ ; in (f) the result for the model III of Gegenbauer moments from [24] is displayed (dashed).

Note that the variations of the form factors calculated from LCSR at different  $q^2$  are strongly correlated, in particular, the shape of the form factor  $f_{B\pi}^+(q^2)$  is correlated with its value at  $q^2 = 0$ . Quoting separate theoretical errors for each point of accessible  $q^2$ -region, including all these correlations makes the numerical predictions too complex and in fact is not necessary, since our main goal is the integrated semileptonic width over this region. Instead, we calculate the deviations of this width with respect to the variations of individual input parameters, so that the correlations are automatically taken into account after the integration over  $q^2$ . Our main result is the integral (2) calculated using the LCSR results for  $f_{B\pi}^+(q^2)$ :

$$\begin{aligned}\Delta\zeta(0, 12 \text{ GeV}^2) &= 4.59 \begin{smallmatrix} +0.16 \\ -0.16 \end{smallmatrix} \Big|_{a2,a4} \begin{smallmatrix} +0.03 \\ -0.03 \end{smallmatrix} \Big|_{m_b} \begin{smallmatrix} +0.68 \\ -0.46 \end{smallmatrix} \Big|_{\mu_\pi} \begin{smallmatrix} +0.31 \\ -0.39 \end{smallmatrix} \Big|_{\mu} \begin{smallmatrix} +0.29 \\ -0.47 \end{smallmatrix} \Big|_{M,s_0} \begin{smallmatrix} +0.59 \\ -0.32 \end{smallmatrix} \Big|_{\bar{M},\bar{s}_0} \text{ps}^{-1} \\ &= 4.59_{-0.85}^{+1.00} \text{ps}^{-1},\end{aligned}\quad (12)$$

where the negligibly small uncertainties related to the rest of the input are not shown but included in the total error obtained by adding all separate uncertainties in quadrature<sup>2</sup>. Importantly, (12) has a slightly smaller overall uncertainty than the values of the form factor  $f_{B\pi}^+(q^2)$  at separate  $q^2$ , due to the abovementioned correlations.

Using (12), we employ the recent BABAR data for the  $B \rightarrow \pi\ell\nu_\ell$  width. The branching fraction integrated from  $q^2 = 0$  to  $q^2 = 12 \text{ GeV}^2$  was measured by the BABAR collaboration using two different techniques, and the results are:

$$\begin{aligned}\Delta\mathcal{B}(0, 12 \text{ GeV}^2) &= (0.84 \pm 0.03 \pm 0.04) \times 10^{-4} \quad [3], \\ \Delta\mathcal{B}(0, 12 \text{ GeV}^2) &= (0.88 \pm 0.06) \times 10^{-4} \quad [2].\end{aligned}\quad (13)$$

Taking their weighted average, the total lifetime  $\tau_{B^0} = 1.525 \pm 0.009 \text{ ps}$  and substituting (12) in (2), we obtain:

$$|V_{ub}| = \left( 3.50_{-0.33}^{+0.38} \Big|_{th.} \pm 0.11 \Big|_{exp.} \right) \times 10^{-3}, \quad (14)$$

where the theoretical error corresponds to the estimated total uncertainty in (12).

## 5 Accessing the large $q^2$ region with z-parameterization

To extrapolate the calculated form factor, we use the  $z$ -series parameterization (see e.g., [14, 30]) based on the analyticity of the form factors and using the transformation:

$$z(q^2, t_0) = \frac{\sqrt{(m_B + m_\pi)^2 - q^2} - \sqrt{(m_B + m_\pi)^2 - t_0}}{\sqrt{(m_B + m_\pi)^2 - q^2} + \sqrt{(m_B + m_\pi)^2 - t_0}}, \quad (15)$$

where  $t_0 = (m_B + m_\pi)^2 - 2\sqrt{m_B m_\pi} \sqrt{(m_B + m_\pi)^2 - q_{min}^2}$  is the auxiliary parameter, chosen to maximally reduce the interval of  $z$  obtained after the mapping (15) of the

---

<sup>2</sup> This replaces our preliminary result  $\Delta\zeta(0, 12 \text{ GeV}^2) = 4.00_{-0.95}^{+1.01}$  quoted in [2, 3] and obtained with exactly the same input as in [12], except no data on  $B \rightarrow \pi\ell\nu_\ell$  were used and broader intervals  $a_2^\pi(1 \text{ GeV}^2) = 0.25 \pm 0.15$  and  $a_4^\pi(1 \text{ GeV}^2) = (0.1 \pm 0.1) - a_2^\pi(1 \text{ GeV}^2)$  were adopted.

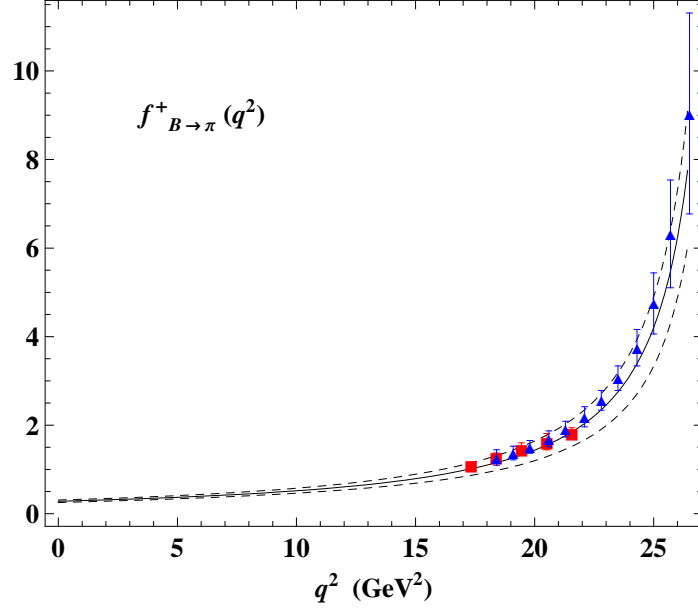


Figure 3: The vector form factor  $f_{B\pi}^+(q^2)$  calculated from LCSR and fitted to the BCL parameterization (solid) with uncertainties (dashed), compared with the HPQCD [5] (squares) and FNAL/MILC [6] (triangles) results.

region  $q_{min}^2 < q^2 < q_{max}^2$ , where the LCSR calculation is valid. More specifically, we adopt the BCL version [14] of this parameterization, that is, for the vector form factor:

$$f_{B\pi}^+(q^2) = \frac{1}{1 - q^2/m_{B^*}^2} \sum_{k=0}^N \tilde{b}_k [z(q^2, t_0)]^k. \quad (16)$$

As explained in [14], this parameterization has certain advantages with respect to the BGL-version [30]. Furthermore, to obey the expected near-threshold behavior, the relation

$$\tilde{b}_N = -\frac{(-1)^N}{N} \sum_{k=0}^{N-1} (-1)^k k \tilde{b}_k \quad (17)$$

is implemented, reducing the number of independent parameters by one. In addition, we find it more convenient to keep the form factor at zero momentum transfer  $f_{B\pi}^+(0)$  as one of the fit parameters, correspondingly rescaling the coefficients in the  $z$ -series expansion. This leads to the same parameterization of the vector form factor as the one

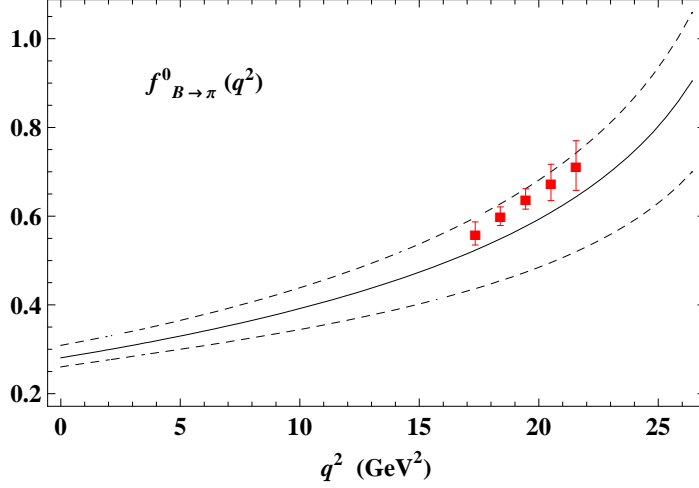


Figure 4: The scalar form factor  $f_{B\pi}^0(q^2)$  calculated from LCSR and fitted to the BCL parameterization. The notations are the same as in Fig. 3.

used in [26]:

$$f_{B\pi}^+(q^2) = \frac{f_{B\pi}^+(0)}{1 - q^2/m_{B^*}^2} \left\{ 1 + \sum_{k=1}^{N-1} b_k \left( z(q^2, t_0)^k - z(0, t_0)^k - (-1)^{N-k} \frac{k}{N} \left[ z(q^2, t_0)^N - z(0, t_0)^N \right] \right) \right\}. \quad (18)$$

The scalar form factor  $f_{B\pi}^0(q^2)$  is parameterized in a similar way, except that there is no pole factor for the obvious reason: the lowest  $B$ -resonance in the  $J^P = 0^+$  channel is located above the  $B\pi$  threshold. Thus, we use:

$$f_{B\pi}^0(q^2) = f_{B\pi}^0(0) \left\{ 1 + \sum_{k=1}^N b_k^0 \left( z(q^2, t_0)^k - z(0, t_0)^k \right) \right\}, \quad (19)$$

where by default  $f_{B\pi}^0(0) = f_{B\pi}^+(0)$ .

We fitted the numerical LCSR prediction for the form factor  $f_{B\pi}^+(q^2)$  to (18) with  $N = 2$  and  $f_{B\pi}^0(q^2)$  to (19) with  $N = 1$ , respectively. To increase the “lever arm” we also employed the LCSR predictions at negative  $q^2$ , up to  $q_{min}^2 = -6.0 \text{ GeV}^2$ . After the mapping (15),  $q_{min}^2 \rightarrow z = 0.30$  and  $q_{max}^2 = 12 \text{ GeV}^2 \rightarrow z = 0.13$ , so that the values of  $z$  are sufficiently small to justify truncating the expansion (16). The number  $N$  of terms in this expansion can be made larger, with no essential change in the fitted form factor but with increasing individual uncertainties for the coefficients  $b_k$  and with large correlations between them. We checked that the upper bounds on the expansion coefficients  $b_k$  following from the OPE of the two-point correlation function of the vector

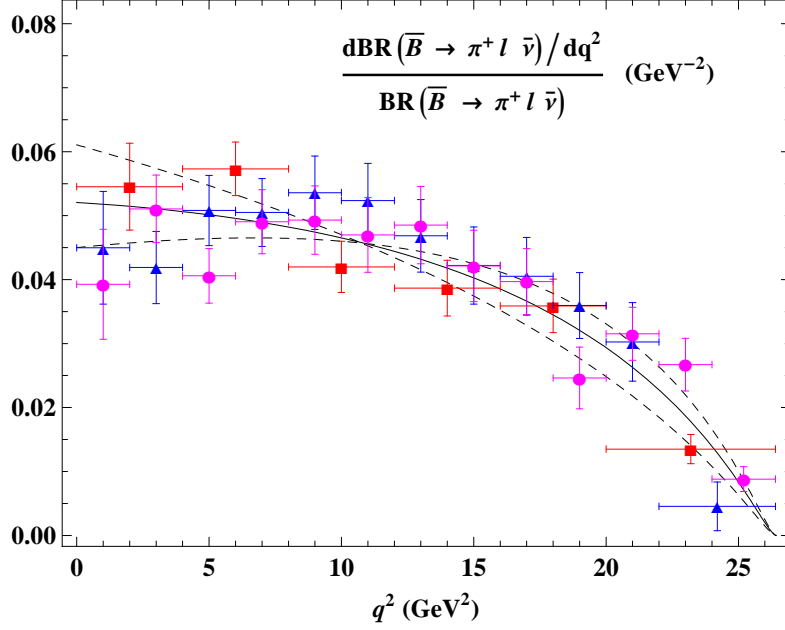


Figure 5: (colour online) The normalized  $q^2$ -distribution in  $B \rightarrow \pi l \nu$  obtained from LCSR and extrapolated with the  $z$ -series parameterization (central input- solid, uncertainties -dashed). The experimental data points are from BABAR: (red) squares [2], (blue) triangles [3] and Belle [4]: (magenta) full circles.

$\bar{b}\gamma_\mu u$  currents (see [14] for detailed expressions) are far from being saturated for low  $N$ . We also used the analogous bounds for the scalar form factor obtained recently in [31]. Altogether, the OPE bounds play a role starting from  $N = 5$ .

The fitted values of  $f_{B\pi}^+(0) = f_{B\pi}^0(0)$  and of the slope parameters  $b_1, b_1^0$  are presented in Table 1, together with the numerically important uncertainties, the latter revealing significant correlations. With these results we extrapolate the form factors at  $q^2 > q_{max}^2$  and compare with the lattice QCD results. This is shown in Fig. 3 for  $f_{B\pi}^+(q^2)$  and in Fig. 4 for  $f_{B\pi}^0(q^2)$ .

The dashed curves in these figures are obtained by adding separate variations of the form factors in quadrature at each  $q^2$ , so that the variations of the solid curves corresponding to the central input are bounded within the area between the upper and lower dashed curves. As expected, the uncertainties of the form factors extrapolated to larger  $q^2$ , exceed the ones calculated at smaller  $q^2$ . This circumstance, however, does not play a significant role for the integrated widths, since the integration over the phase space suppresses the semileptonic width in the large  $q^2$ -region.

Our predictions for  $f_{B\pi}^+$  are, within errors, in a reasonable agreement with the lattice QCD results obtained by HPQCD [5] and Fermilab/MILC [6] collaborations. We also observe an agreement with the normalization and shape of the form factors obtained by the QCDSF collaboration [7], in particular, they predict  $f_{B\pi}^+(0) = 0.27 \pm 0.07 \pm 0.05$ .

| Parameter       | centr. value | $\{a_2, a_4\}$       | $\mu_\pi$            | $\mu$                | $\{M^2, s_0\}$       | $\{\overline{M}^2, \overline{s}_0\}$ |
|-----------------|--------------|----------------------|----------------------|----------------------|----------------------|--------------------------------------|
| $f_{B\pi}^+(0)$ | 0.281        | $+0.002$<br>$-0.003$ | $+0.018$<br>$-0.014$ | $-0.005$<br>$+0.008$ | $+0.010$<br>$-0.022$ | $-0.010$<br>$+0.016$                 |
| $b_1$           | -1.62        | $+0.43$<br>$-0.44$   | $-0.06$<br>$+0.05$   | $+0.53$<br>$-0.07$   | $+0.30$<br>$-0.49$   | -                                    |
| $b_1^0$         | -3.98        | $+0.56$<br>$-0.57$   | $-0.28$<br>$+0.23$   | $+0.96$<br>$-0.08$   | $+0.28$<br>$-0.42$   | -                                    |

Table 1: *Fitted parameters for  $z$ -series parameterization of the form factors  $f_{B\pi}^{+,0}(q^2)$  and their uncertainties due to the variations of the input parameters.*

Furthermore, we estimate the total width of  $B \rightarrow \pi\ell\nu_\ell$  in units of  $1/|V_{ub}|^2$  and the integral (2) for the large  $q^2$ -region:

$$\frac{1}{|V_{ub}|^2}\Gamma(B \rightarrow \pi\ell\nu_\ell) = \Delta\zeta(0, 26.4 \text{ GeV}^2) = 7.71_{-1.61}^{+1.71} \text{ ps}^{-1},$$

$$\Delta\zeta(16 \text{ GeV}^2, 26.4 \text{ GeV}^2) = 1.88_{-0.59}^{+0.53} \text{ ps}^{-1}. \quad (20)$$

Our prediction for the latter integral has to be compared with the lattice QCD results presented below, in Table 2.

In Fig. 5 we plot the predicted  $q^2$ -shape in  $B \rightarrow \pi\ell\nu_\ell$  obtained by calculating the normalized differential width  $(1/\Gamma)d\Gamma/dq^2$  from LCSR at  $0 \leq q^2 \leq q_{max}^2$  and from the  $z$ -series parameterization at  $q_{max}^2 < q^2 \leq (m_B - m_\pi)^2$ . The estimated uncertainties are naturally smaller than in Fig 3, because the variations of the form factor normalization cancel in the ratio of the differential and total widths. Our result is compared with the measured  $q^2$ -distributions. We use the partial  $\Delta\mathcal{B}$  spectrum obtained by the BABAR collaboration in 6 bins and 12 bins from the two independent analyses [2] and [3], respectively. For the normalization we employ the corresponding central values of the measured total branching fractions:  $\mathcal{B}(B^0 \rightarrow \pi^-\ell^+\nu_\ell) = (1.41 \pm 0.05 \pm 0.07) \times 10^{-4}$  [2] and  $\mathcal{B}(B^0 \rightarrow \pi^-\ell^+\nu_\ell) = (1.42 \pm 0.05 \pm 0.07) \times 10^{-4}$  [3]. The analogous 13-bin distribution measured by the Belle collaboration [4] and normalized by their total branching fraction  $\mathcal{B}(B^0 \rightarrow \pi^-\ell^+\nu_\ell) = (1.49 \pm 0.04 \pm 0.07) \times 10^{-4}$  is also shown. Fig. 5 reveals a general agreement of our prediction for the  $q^2$ -shape and experimental results, however, only within still large uncertainties of both experiment and theory. In particular, the shape of the form factor fitted from the BABAR data in [2] to the same BCL parameterization with two parameters yields:  $(\tilde{b}_1/\tilde{b}_0)_{BABAR} = -0.67 \pm 0.18$ , whereas our result for the same ratio is  $(\tilde{b}_1/\tilde{b}_0)_{LCSR} = -1.10_{-0.27}^{+0.40}$ .

A “byproduct” observable that was not yet measured in  $B \rightarrow \pi\ell\nu_\ell$ , is the distribution of the lepton energy in the  $B$ -meson rest frame shown in Fig. 6 in the normalized form. In the electron or muon semileptonic  $B$ -decay, at a given lepton energy, the distribution  $d\Gamma(B \rightarrow \pi\ell\nu_\ell)/dE_\ell$  contains the integral of  $|f_{B\pi}^+(q^2)|^2$  over the region  $0 < q^2 \lesssim 2m_BE_\ell$  (the expression for this distribution, also at  $m_\ell \neq 0$ , can be found, e.g., in [32]). Hence

the correlations between the normalization and shape of the form factor somewhat reduce the uncertainties in this distribution. It also has a more pronounced slope than the  $q^2$  distribution.

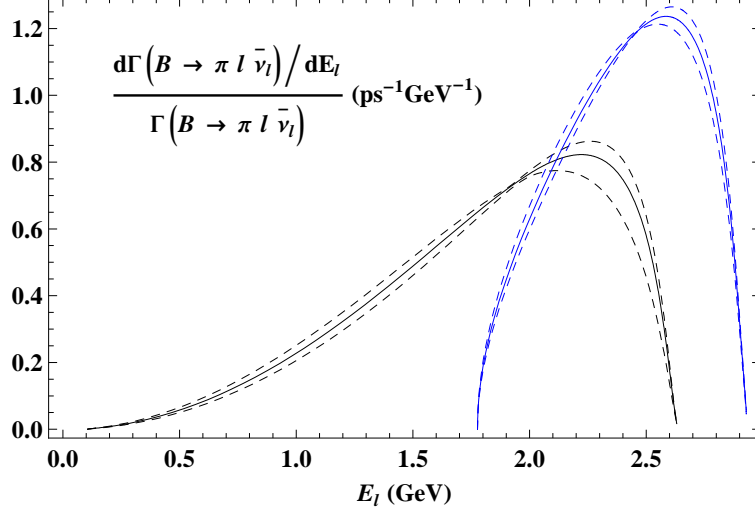


Figure 6: *Lepton energy spectra for  $B \rightarrow \pi l \bar{\nu}_l$  at  $m_\ell \leq E_\ell \lesssim (m_B^2 + m_\ell^2)/(2m_B)$  for  $\ell = \mu, \tau$ . Solid (dashed) lines correspond to the form factors calculated at the central input (indicate the uncertainties).*

## 6 $B \rightarrow \tau \nu_\tau$ and $B \rightarrow \pi \tau \nu_\tau$

Currently, the leptonic width  $B \rightarrow \tau \nu_\tau$  measured by both BABAR and Belle collaborations (see Table 2) is larger than the SM prediction:

$$\mathcal{B}(B^- \rightarrow \tau \bar{\nu}_\tau) = \frac{G_F^2}{8\pi} |V_{ub}|^2 m_\tau^2 m_B \left(1 - \frac{m_\tau^2}{m_B^2}\right)^2 f_B^2 \tau_{B^-}, \quad (21)$$

if one employs  $f_B$  predicted from lattice QCD or QCD sum rules, together with  $|V_{ub}|$  extracted from  $B \rightarrow \pi l \nu_\ell$ . The recent discussions on this situation are mostly concentrated on the value of  $|V_{ub}|$ . Indeed, the tension decreases, if one uses in (21) the somewhat larger value of  $|V_{ub}|$  extracted from the inclusive  $b \rightarrow u$  decays. On the other hand, the CKM fits [33, 34] yield a smaller  $|V_{ub}|$ , consistent with the determinations from  $B \rightarrow \pi l \nu_\ell$ .

Let us emphasize that, independent of the actual  $|V_{ub}|$  value, there exists a tension between the ratio of semileptonic and leptonic  $B$  widths and the QCD predictions for the two relevant hadronic matrix elements  $f_{B\pi}^+(q^2)$  and  $f_B$ . To demonstrate that, we define the following observable:

$$R_{s/l}(q_1^2, q_2^2) \equiv \frac{\Delta \mathcal{B}_{B \rightarrow \pi l \nu_\ell}(q_1^2, q_2^2)}{\mathcal{B}(B \rightarrow \tau \nu_\tau)} \left( \frac{\tau_{B^-}}{\tau_{B^0}} \right) = \frac{\Delta \zeta(q_1^2, q_2^2)}{(G_F^2/8\pi) m_\tau^2 m_B (1 - m_\tau^2/m_B^2)^2 f_B^2}, \quad (22)$$

where the partial branching fraction  $\Delta\mathcal{B}$  and the integral  $\Delta\zeta$  defined as in (2), are taken over the same region  $q_1^2 \leq q^2 \leq q_2^2$  of the momentum transfer.

The above equation for the ratio  $R_{s/l}$  follows solely from the  $V - A$  structure of the weak currents in SM and  $V_{ub}$  cancels out in the ratio. The form factor  $f_{B\pi}^+$  and decay constant  $f_B$  entering r.h.s. are obtained by one and the same QCD method: lattice QCD or the combination of LCSR and QCD sum rule. In Tables 2 and 3 we collect the inputs for this equation, obtained from different measurements and QCD calculations. The disagreement between the calculated and measured ratio  $R_{s/l}$  goes beyond the theoretical and experimental errors, especially in the case of the lattice calculations which have smaller uncertainties.

| Exp.      | $\Delta\mathcal{B}(10^{-4})$ [Ref.]                 | $\mathcal{B}(B \rightarrow \tau\nu_\tau)(10^{-4})$ [Ref.] | $R_{s/l}$              |
|-----------|---|---|------------------------|
| BABAR     | $0.32 \pm 0.03$ [2]<br>$0.33 \pm 0.03 \pm 0.03$ [3] | $1.76 \pm 0.49$ [37, 38]                                  | $0.20^{+0.08}_{-0.05}$ |
| Belle     | $0.398 \pm 0.03$ [4]                                | $1.54^{+0.38+0.29}_{-0.37-0.31}$ [39]                     | $0.28^{+0.13}_{-0.07}$ |
| QCD       | $\Delta\zeta(\text{ps}^{-1})$ [Ref.]                | $f_B(\text{MeV})$ [Ref.]                                  | $R_{s/l}$              |
| HPQCD     | $2.02 \pm 0.55$ [5]                                 | $190 \pm 13$ [35]   | $0.52 \pm 0.16$        |
| FNAL/MILC | $2.21^{+0.47}_{-0.42}$ [6]                          | $212 \pm 9$ [36]  | $0.46 \pm 0.10$        |

Table 2: The ratio  $R_{s/l}$  for the region  $16 \text{ GeV}^2 < q^2 < 26.4 \text{ GeV}^2$ , measured and calculated from (22) using the lattice QCD results. The weighted average over the two BABAR measurements is taken and all errors are added in quadrature.

Decreasing further the theoretical and experimental errors in (22), especially in the  $B \rightarrow \tau\nu_\tau$  width, becomes therefore a very important task. Possible effects beyond the SM in  $B \rightarrow \tau\nu_\tau$  are already being discussed in the literature, and, in particular,  $B \rightarrow D\tau\nu_\tau$  is proposed as a channel which has common new physics contributions with the leptonic  $B$  decay (see e.g., [40] and references therein).

Here we would like to attract attention to another semileptonic channel:  $B \rightarrow \pi\tau\nu_\tau$ , although it is experimentally very demanding. Earlier this channel was discussed e.g., in [32, 41]. Note that this channel has the same combination of quark and lepton flavours as  $B \rightarrow \tau\nu_\tau$ . In the SM, the  $B \rightarrow \pi\tau\nu_\tau$  decay differs only kinematically from the semileptonic modes with the muon or electron. A convenient,  $V_{ub}$ -independent



| Exp.       | $\Delta\mathcal{B}(10^{-4})$ [Ref.]                 | $\mathcal{B}(B \rightarrow \tau\nu_\tau)(10^{-4})$ [Ref.] | $R_{s/l}$              |
|------------|---|---|------------------------|
| BABAR      | $0.88 \pm 0.06$ [2]<br>$0.84 \pm 0.03 \pm 0.04$ [3] | $1.76 \pm 0.49$ [37, 38]                                  | $0.52^{+0.20}_{-0.12}$ |
| QCD        | $\Delta\zeta$ [Ref.]                                | $f_B(\text{MeV})$ [Ref.]                                  | $R_{s/l}$              |
| LCSR/QCDSR | $4.59^{+1.00}_{-0.85}$ [this work]                  | $210 \pm 19$ [42]   | $0.97^{+0.28}_{-0.24}$ |

Table 3: The same as in Table 2 for the region  $0 \leq q^2 \leq 12.0 \text{ GeV}^2$  where the QCD sum rule results are used.

observable [43] is the ratio

$$\frac{d\Gamma(B \rightarrow \pi\tau\nu_\tau)/dq^2}{d\Gamma(B \rightarrow \pi\ell\nu_\ell)/dq^2} = \frac{(q^2 - m_\tau^2)^2}{(q^2)^2} \left(1 + \frac{m_\tau^2}{2q^2}\right) \times \left\{1 + \frac{3m_\tau^2(m_B^2 - m_\pi^2)^2}{4(m_\tau^2 + 2q^2)m_B^2 p_\pi^2} \frac{|f_{B\pi}^0(q^2)|^2}{|f_{B\pi}^+(q^2)|^2}\right\}, \quad (23)$$

where  $\ell = e$  or  $\mu$  and  $m_\ell$  is neglected. It is determined by the ratio of the scalar and vector  $B \rightarrow \pi$  form factors, hence, it has a somewhat smaller uncertainty than the individual form factors. The ratio (23) is plotted in Fig. 8 in the kinematically allowed region  $m_\tau^2 < q^2 < (m_B - m_\pi)^2$ , using our predictions for the form factors. It grows at large  $q^2$ , due to the kinematical suppression of the vector channel contribution at small  $p_\pi$ . The strong correlations between the vector and scalar form factors calculated from LCSR with one and the same input result in a small uncertainty in their ratio. The tau-lepton energy spectrum for  $B \rightarrow \pi\tau\nu$  shown in Fig. 6 is another observable which depends on both vector and scalar form factors.

To investigate the influence of new physics on both leptonic and semileptonic  $B$  decays with a  $\tau$ -lepton, we include in the effective Hamiltonian of the  $b \rightarrow u\tau\nu_\tau$  transition an intermediate charged Higgs-boson contribution adopted in the same generic form as in [40] :

$$H_{eff} = \frac{G_F}{\sqrt{2}} V_{ub} \left\{ \bar{u} \gamma_\mu (1 - \gamma_5) b \bar{\tau} \gamma^\mu (1 - \gamma_5) \nu_\tau - \frac{\bar{m}_b m_\tau}{m_B^2} \bar{u} \left( g_S + g_P \gamma_5 \right) b \bar{\tau} (1 - \gamma_5) \nu_\tau \right\} + h.c., \quad (24)$$

The admixture of new physics in  $B \rightarrow \tau\nu_\tau$  and  $B \rightarrow \pi\tau\nu_\tau$  is then determined, respectively, by the pseudoscalar and scalar parts of the new interaction. In particular, the leptonic width (21) gets multiplied by  $(1 - g_P)^2$ ; and therefore, with this choice, the

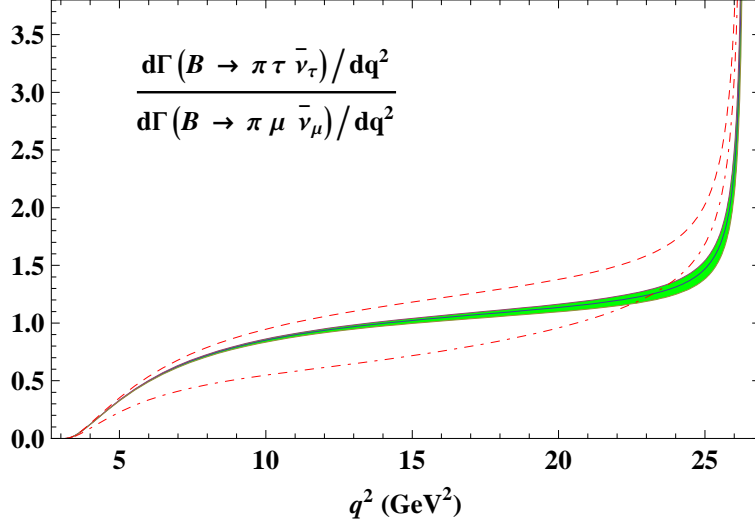


Figure 7: (colour online) Ratio of differential decay widths, defined in (23) (solid), with shaded (green) area indicating the uncertainties. Also shown is the effect of adding a charged Higgs-boson contribution with  $g_S = -0.4$  (dashed, red) and  $g_S = 2.4$  (dash-dotted, red)

$B \rightarrow \tau \nu_\tau$  width vanishes at  $g_P = 1$ . Accordingly, the r.h.s. of (22) acquires a factor  $1/(1 - g_P)^2$ . Also the ratio (23) is modified by multiplying the scalar form factor with an additional factor:

$$f_{B\pi}^0(q^2) \rightarrow \left(1 - \frac{g_S q^2}{m_B^2}\right) f_{B\pi}^0(q^2), \quad (25)$$

The addition of the new interaction can fill the gap between the calculated and experimentally measured ratio  $R_{s/l}$  in (22) if one allows for  $g_P \neq 0$ . Taking, e.g., the sum rule prediction for this ratio from Table 3, and adding the new physics contribution,  $R_{s/l} \rightarrow R_{s/l}/(1 - g_P)^2$ , we equate it to the experimental value and find that  $g_P \neq 0$  is allowed within one of the following two intervals:  $g_P = -(0.4 \pm 0.2|_{th} \pm 0.2|_{exp})$  or  $g_P = 2.4 \pm 0.2|_{th} \pm 0.2|_{exp}$ . Assuming the parameter  $g_S$  in the same ballpark as  $g_P$  (in fact,  $g_S = g_P$  in MSSM, however, only with positive values), we display in Fig. 7 the modified ratio (23), adding the new physics contribution with  $g_S = -0.4$  and  $g_S = 2.4$ . In fact, the second option may already be excluded by the  $B \rightarrow D\tau\nu_\tau$  analysis (see e.g., [44]). In addition, in Fig. 8, the ratio of total semileptonic widths is plotted as a function of  $g_S$ . Note that the deviation due to new physics can be larger than the uncertainty due to the hadronic form factors.

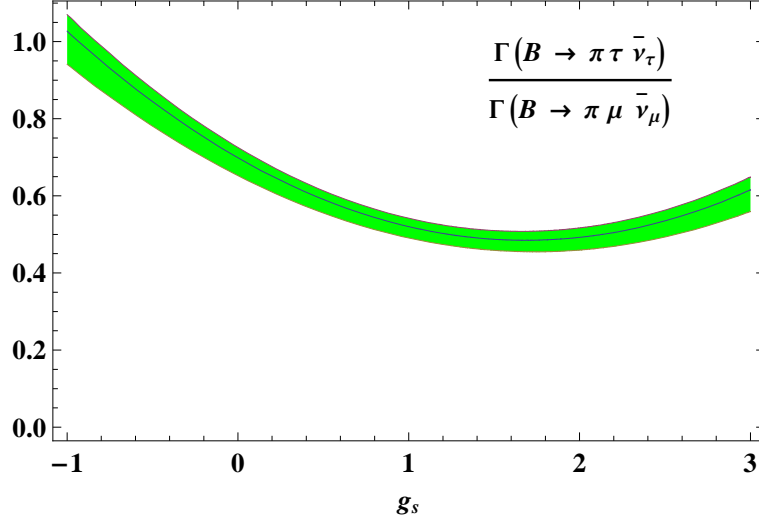


Figure 8: *Ratio of total semileptonic decay widths into  $\tau$  and  $\mu$  (or  $e$ ) (solid), with shaded (green) area indicating the uncertainties shown as a function of the parameter  $g_s$  determining the charged Higgs-boson coupling in  $B \rightarrow \pi \tau \nu_\tau$*

## 7 Discussion

The precise determination of the CKM matrix element  $V_{ub}$  is mandatory for stringent tests of the quark-flavour content of SM. Due to recent work in lattice QCD and in QCD sum rules, combined with constraints from analyticity and unitarity, the values for  $|V_{ub}|$  extracted from  $B \rightarrow \pi \ell \bar{\nu}$  are becoming quite precise. The main result of this paper is the prediction for the partial width of this decay in the  $q^2$ -region  $0 \leq q^2 \leq 12 \text{ GeV}^2$  in terms of  $1/|V_{ub}|^2$ , which is expressed as a weighted integral  $\Delta\zeta(0, 12 \text{ GeV}^2)$  over the squared form factor  $f_{B\pi}^+(q^2)$ . This integral has smaller uncertainties than the values of the form factor at separate  $q^2$  and allows the  $|V_{ub}|$  extraction with an accuracy approaching 10%, somewhat better than in the previous LCSR analysis [12] where only the value of the form factor at  $q^2 = 0$  was used. We extract a value for  $|V_{ub}|$  using recent BABAR data [2, 3]. We hope that also the Belle collaboration will in future provide the integrated width in this region.

We also employed the  $z$ -series parameterization with BCL-ansatz and extrapolated the LCSR form factors to the whole kinematic region. The  $B \rightarrow \pi$  form factors  $f_{B\pi}^+(q^2)$  and  $f_{B\pi}^0(q^2)$  obtained from LCSR are, within comparable uncertainties, in agreement with the recent lattice QCD results and with the measured  $q^2$ -shape of the  $B \rightarrow \pi \ell \nu_\ell$  width. A combined fit of the form factors calculated at small  $q^2$  from LCSR and at large  $q^2$  from lattice QCD to a common  $z$ -series parameterization is possible (see e.g. the previous analysis in [14]) but is beyond the scope of this paper.

A further improvement would need more precise measurements of the shape to control the input parameters used in LCSR. On the theoretical side, the renormalization

scale dependence can be reduced by including NNLO corrections to the hard scattering amplitudes, and also by separating the renormalization and the factorization scales. Improving the duality approximation is more difficult and demands a knowledge of radially excited states in  $B$  channel. Another perspective is a simultaneous global fit of three different LCSR's to the data on  $B \rightarrow \pi \ell \nu_\ell$  and on the pion electromagnetic and transition form factors, with scanning over the allowed region of input.

The value for  $|V_{ub}|$  obtained from  $B \rightarrow \pi \ell \nu_\ell$  is somewhat lower than what is extracted from inclusive  $B$  decays, as well as the one extracted from  $B \rightarrow \tau \bar{\nu}$ , but the significance is still too small to be conclusive. On the other hand, our result is completely compatible with the results from the CKM fits [33, 34].

The impact of the recent measurements of  $B \rightarrow \tau \bar{\nu}$  on  $V_{ub}$  has not improved the situation concerning our knowledge of this quantity. However, the ratio of leptonic and semileptonic widths is independent of  $V_{ub}$  and may either be regarded as a test for a possible non-standard contribution (like, e.g. a charged Higgs-boson exchange) or as a test of our understanding of QCD. In turn, a lack of understanding of  $f_B$  and the form factor  $f_{B\pi}^+$  will severely limit the sensitivity to a “new physics” contribution. It is interesting to note that both QCD sum rules as well as lattice calculations tend to yield larger values of a suitably defined ratio of semileptonic versus leptonic widths. This means that we have either a problem in our understanding of QCD matrix elements or that there is really a substantial new-physics contribution in  $B \rightarrow \tau \bar{\nu}$ , which also makes the channel  $B \rightarrow \pi \tau \nu_\tau$  very interesting. A significant test of these statements has to await more data, in particular on  $B \rightarrow \tau \bar{\nu}$ .

## Acknowledgments

We are grateful to Martin Jung and Christoph Klein for useful comments and acknowledge valuable discussions concerning the BABAR collaboration data with Jochen Dingfelder and Paul Taras. This work is supported by the German research foundation DFG under the contract No. KH205/1-2 and by the German Ministry of Research (BMBF), contract 05H09PSF.

## References

- [1] R. Kowalewski and Th. Mannel, “Determination of  $V_{cb}$  and  $V_{ub}$ ”, in K. Nakamura *et al.* [Particle Data Group], J. Phys. G **37** (2010) 075021, pp. 951-965.
- [2] P. del Amo Sanchez *et al.* [BABAR Collaboration], Phys. Rev. D **83** (2011) 032007.
- [3] P. del Amo Sanchez *et al.* [BABAR Collaboration], arXiv:1010.0987 [hep-ex].
- [4] H. Ha *et al.*, arXiv:1012.0090 [hep-ex].
- [5] E. Gulez *et al.* Phys. Rev. D **73** (2006) 074502 [Erratum-ibid. D **75** (2007) 119906].
- [6] J. A. Bailey *et al.*, Phys. Rev. D **79** (2009) 054507.

- [7] A. Al-Haydari *et al.* [QCDSF Collaboration], Eur. Phys. J. A **43** (2010) 107.
- [8] A. Khodjamirian, R. Ruckl, S. Weinzierl and O. I. Yakovlev, Phys. Lett. B **410** (1997) 275.
- [9] E. Bagan, P. Ball and V. M. Braun, Phys. Lett. B **417** (1998) 154.
- [10] P. Ball, JHEP **9809** (1998) 005.
- [11] P. Ball and R. Zwicky, Phys. Rev. D **71** (2005) 014015.
- [12] G. Duplancic, A. Khodjamirian, T. Mannel, B. Melic and N. Offen, JHEP **0804**, 014 (2008).
- [13] B. Aubert *et al.* [BABAR Collaboration], Phys. Rev. Lett. **98** (2007) 091801.
- [14] C. Bourrely, I. Caprini and L. Lellouch, Phys. Rev. D **79** (2009) 013008.
- [15] P. Ball, V. M. Braun and A. Lenz, JHEP **0605** (2006) 004.
- [16] V. M. Braun and I. E. Halperin, Phys. Lett. B **328** (1994) 457.
- [17] V. M. Braun, A. Khodjamirian and M. Maul, Phys. Rev. D **61** (2000) 073004.
- [18] J. Bijnens and A. Khodjamirian, Eur. Phys. J. C **26** (2002) 67.
- [19] G. M. Huber *et al.* [Jefferson Lab Collaboration], Phys. Rev. C **78** (2008) 045203.
- [20] A. Khodjamirian, Int. J. Mod. Phys. A **25**, 513 (2010) [arXiv:0909.2154 [hep-ph]].
- [21] V. M. Braun *et al.*, Phys. Rev. D **74** (2006) 074501;  
R. Arthur *et al.*, arXiv:1011.5906 [hep-lat].
- [22] A. Khodjamirian, T. Mannel and M. Melcher, Phys. Rev. D **70**, 094002 (2004).
- [23] A. Khodjamirian, Eur. Phys. J. C **6**, 477 (1999).
- [24] S. S. Agaev, V. M. Braun, N. Offen and F. A. Porkert, arXiv:1012.4671 [hep-ph].
- [25] B. Aubert *et al.* [ The BABAR Collaboration ], Phys. Rev. **D80** (2009) 052002.
- [26] A. Khodjamirian, C. Klein, T. Mannel and N. Offen, Phys. Rev. D **80**, 114005 (2009).
- [27] K. G. Chetyrkin, J. H. Kühn, A. Maier *et al.*, Phys. Rev. **D80** (2009) 074010;  
K. Chetyrkin, J. H. Kuhn, A. Maier, P. Maierhofer, P. Marquard, M. Steinhauser,  
C. Sturm, [arXiv:1010.6157 [hep-ph]].
- [28] K. G. Chetyrkin and A. Khodjamirian, Eur. Phys. J. C **46** (2006) 721;  
M. Jamin, J. A. Oller and A. Pich, Phys. Rev. D **74** (2006) 074009.
- [29] H. Leutwyler, Phys. Lett. B **378**, 313 (1996).

- [30] C. G. Boyd, B. Grinstein and R. F. Lebed, Phys. Rev. Lett. **74** (1995) 4603; Phys. Lett. B **353** (1995) 306.
- [31] A. Bharucha, T. Feldmann and M. Wick, JHEP **1009** (2010) 090.
- [32] A. Khodjamirian and R. Rückl, Adv. Ser. Direct. High Energy Phys. **15** (1998) 345 [arXiv:hep-ph/9801443].
- [33] J. Charles *et al.* [CKMfitter Group], Eur. Phys. J. C **41** (2005) 1, <http://ckmfitter.in2p3.fr>;
- [34] A. J. Bevan *et al.* [UTfit Collaboration] arXiv:1010.5089 [hep-ph], <http://www.utfit.org/UTfit> .
- [35] E. Gamiz, C. T. H. Davies, G. P. Lepage, J. Shigemitsu and M. Wingate [HPQCD Collaboration], Phys. Rev. D **80** (2009) 014503.
- [36] J. Simone *et al.* [Fermilab Lattice and MILC Collaborations], PoS **LAT-TICE2010**, 317 (2010).
- [37] P. del Amo Sanchez *et al.* [BABAR Collaboration], arXiv:1008.0104 [hep-ex].
- [38] R. Barlow, arXiv:1102.1267 [hep-ex].
- [39] K. Hara *et al.* [Belle collaboration], Phys. Rev. D **82** (2010) 071101.
- [40] U. Nierste, S. Trine, S. Westhoff, Phys. Rev. **D78** (2008) 015006.
- [41] C. A. Dominguez, J. G. Körner and K. Schilcher, Phys. Lett. B **248** (1990) 399.
- [42] M. Jamin and B. O. Lange, Phys. Rev. D **65**, 056005 (2002).
- [43] A. Khodjamirian, PoS **BEAUTY2009** (2009) 045.
- [44] M. Jung, A. Pich and P. Tuzon, JHEP **1011** (2010) 003;  
O. Deschamps, S. Descotes-Genon, S. Monteil, V. Niess, S. T’Jampens and V. Tisserand, Phys. Rev. D **82** (2010) 073012.